



# VIBRO-ACOUSTIC COUPLING ANALYSIS FOR HARMONIC SOUND PLATE

Bor-Tsuen Wang, Chia-Hsien Huang

*National Pingtung University of Science and Technology, Dept. of Mech. Eng., 912, Pingtung, Taiwan*  
email: wangbt@mail.npust.edu.tw

Ying-Hui Wu

*Machinery Division, National Nei-Pu Senior Agricultural-Industrial Vocational School, 912, Pingtung, Taiwan*

Harmonic sound plate (HSP) with a special shape that can produce percussion sound with several harmonic overtones has been developed. This work aims to present the simulation of radiated sound response from the HSP. Both structural field analysis and structure-acoustic field analysis considering air-structure coupling effect will be conducted. The solid elements are used to construct the HSP structure model, and the acoustic field elements are used to simulate the surrounding air. Theoretical modal analysis is first performed to obtain structural natural frequencies and displacement mode shapes for structure only, while the acoustic field mode shapes, i.e. sound pressure mode shapes in the air, can be obtained in air-structure coupling analysis. Harmonic response analysis is also carried out to obtain the radiated percussion sound response in the air due to the impact force. Results show the air-structure interaction has a slight effect on structural natural frequencies. Both structural mode shapes and acoustic mode shapes can be visualized to interpret the sound pressure response of HSP experimentally and theoretically. The predicted radiated sound can be useful and further applied to evaluate the percussion sound quality.

---

## 1. Introduction

Percussion instruments are widely used in musical performance. Different percussion instruments have different sound characteristics, in particular related to structural vibration modes. Harmonic sound plate (HSP) with the uniform thickness and curved shape has been developed as a new type of percussion instrument [1]. This work aims to perform vibro-acoustic analysis on the HSP in air-surrounding so as to predict the radiated sound pressure.

McLachlan et al. [2] adopted finite element analysis (FEA) to design the musical bells containing up to seven overtone frequencies in the harmonic series. McLachlan et al. [3] developed the folded octagonal gong made of laser cut sheet metal for folding into the gong that can produce the first five overtones tuned to within 5% of the harmonic sound. Pan [4] investigated ancient Chinese musical bells and found the diamond shape of cross section incurred two different axisymmetric modes. The normal strike and side strike will generate two different major spectral notes of sound. Yoo and Rossing [5] constructed the finite element model to determine structural natural frequencies and their mode shapes for both Chinese and Korean stone chimes. The analytical model is applied to systematically vary the vertex angle and base line of the chime for exploring the difference of percussion sound.

Since the percussion sound is of interest, the simulation technique to analytically obtain the radiated sound pressure distribution from the structure has been drawn attention. Liu and Yi [6] applied

commercial software to examine the effect of vibro-acoustic on acoustic natural frequencies, acoustic pressure and structural response for a flexible thin shell with a cylinder-like cavity. Wang et al. [7, 8] have developed analytical and experimental approaches in studying special types of percussion instruments, such as the steel chime [7] and crotale [8], respectively. The structural modal parameters for structure-only and air-structure systems are investigated. Results show the predicted natural frequencies agree very well in comparison to the experimental results.

This work will present both the structure-only and air-structural system analysis in particular for the HSP. For modal analysis, the system modal parameters can be obtained, while the system frequency response function (FRF) can be determined from harmonic response analysis. The differences of modal characteristics for both the structure-only and air-structure systems will be discussed, respectively. The simulation of sound field analysis to predict the radiated sound pressure distribution from the HSP can be useful for evaluating the percussion sound quality analytically.

## 2. Theoretical formulation for vibro-acoustic analysis

Fig. 1(a) shows the system block diagram of air-structure system in physical domain. The dotted line block in Fig. 1(a) represents the structure-only system which equations can be expressed as follows:

$$[M_s]\{\ddot{u}\} + [C_s]\{\dot{u}\} + [K_s]\{u\} = \{F_s\} + [R]\{p\}. \quad (1)$$

where  $[M_s]$ ,  $[C_s]$ ,  $[K_s]$  and  $[R]$  are the structural mass, damping, stiffness and vibro-acoustic coupling matrices, respectively;  $\{u\}$ ,  $\{\dot{u}\}$ , and  $\{\ddot{u}\}$  are the displacement, velocity, and acceleration vector on the structure;  $\{p\}$  is the acoustic pressure vector. The  $[R]$  term in Eq. (1) is not effective for the structure-only system.

The air-path system equations can be expressed as follows:

$$[M_f]\{\ddot{p}\} + [C_f]\{\dot{p}\} + [K_f]\{p\} = \{F_f\} - \rho_0[R]^T\{\ddot{u}\}. \quad (2)$$

where  $[M_f]$ ,  $[C_f]$  and  $[K_f]$  are the air (fluid) mass, damping and stiffness matrices, respectively;  $\rho_0$  is the air density, and the associate term represents the air-structure interface loading to the air;  $\{F_f\}$  is the acoustic loading vector. The integrated fluid-structure system equation can be derived as follows:

$$\begin{bmatrix} [M_s] & 0 \\ \rho_0[R]^T & [M_f] \end{bmatrix} \begin{Bmatrix} \{\ddot{u}\} \\ \{\ddot{p}\} \end{Bmatrix} + \begin{bmatrix} [C_s] & 0 \\ 0 & [C_f] \end{bmatrix} \begin{Bmatrix} \{\dot{u}\} \\ \{\dot{p}\} \end{Bmatrix} + \begin{bmatrix} [K_s] & -[R] \\ 0 & [K_f] \end{bmatrix} \begin{Bmatrix} \{u\} \\ \{p\} \end{Bmatrix} = \begin{Bmatrix} \{F_s\} \\ \{F_f\} \end{Bmatrix}, \quad (3)$$

or in the simple expression:

$$[M]\{\ddot{x}\} + [C]\{\dot{x}\} + [K]\{x\} = \{f\}. \quad (4)$$

For the structure-only system, the  $[R]$  term in Eq. (1) can be ignored such that Eq. (1) has the same form as Eq. (4). For harmonic response analysis, the harmonic solutions of  $\{f\} = \{F\}e^{i\omega t}$ ,  $\{u\} = \{U\}e^{i\omega t}$  and  $\{p\} = \{P\}e^{i\omega t}$  can be assumed and so forth the system equations can be formulated as follows:

$$\left[ ([K] - \omega^2[M]) \right] \{X\} + i\omega[C]\{X\} = \{F\}. \quad (5)$$

where  $\omega = 2\pi f$ .  $\omega$  is the frequency in rad/sec and  $f$  in Hz. By ignoring the force vector and neglecting damping term, the undamped structure-only system natural frequencies  $f_r$  and corresponding mode shapes  $\phi_{r(s)}$ , or simply denoted  $\phi_r$ , can be obtained as shown in Fig. 1(b). Note that the modal damping ratio  $\zeta_r$  can only be determined from experiments. If the air-structure system is

considered, the system modal parameters are shown as  $\bar{f}_r$ ,  $\bar{\phi}_r$  and  $\bar{\zeta}_r$ , respectively. It is noted that both the structure-only natural frequency  $f_r$  and the air-structure natural frequency  $\bar{f}_r$  are different theoretically. While  $\phi_r$  designates the structural displacement mode shape,  $\bar{\phi}_r$  is referred to the air-structure system mode shapes that can contain the structural displacement mode shape  $\bar{\phi}_{r(s)}$  and the air acoustic mode shape  $\bar{\phi}_{r(a)}$ , i.e., the radiated sound pressure mode shape.

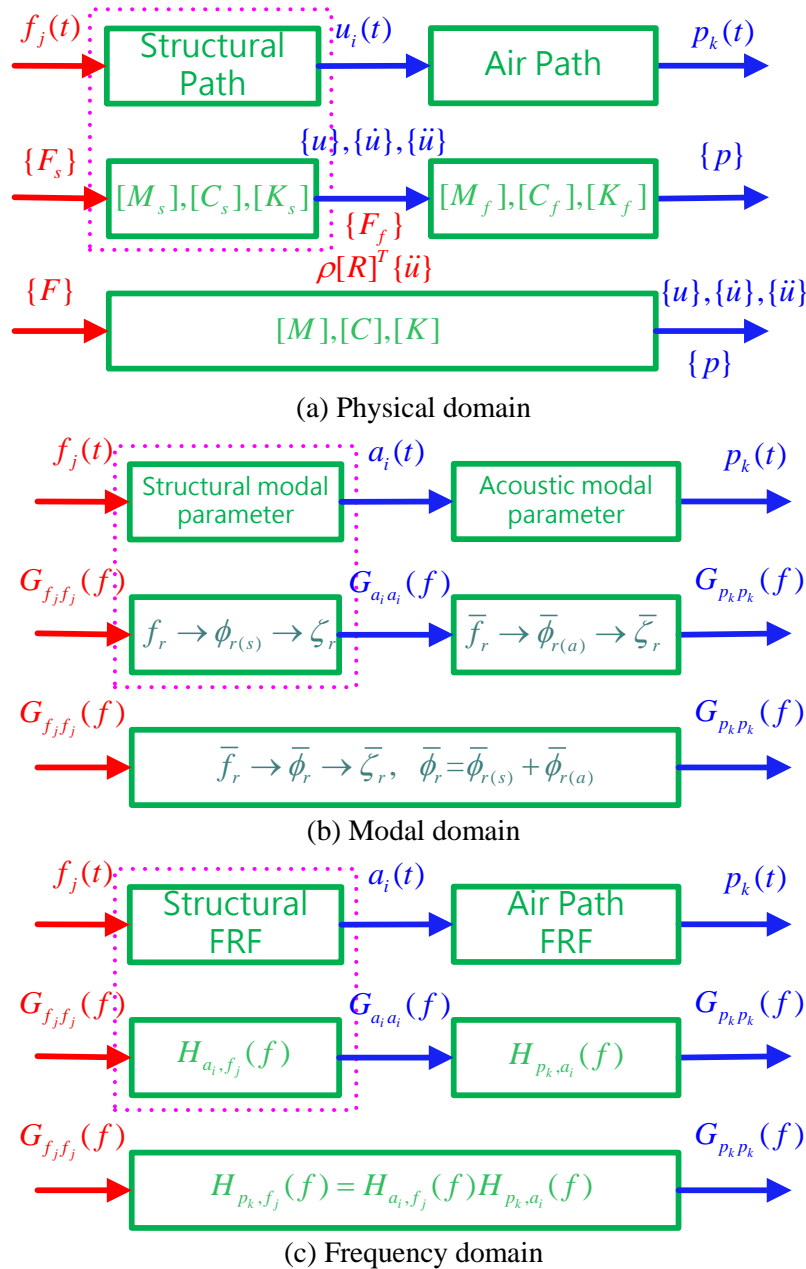


Figure 1: System block diagram of air-structure field analysis.

Referring to Fig. 1(c) in the aspect of frequency domain, one can measure the acceleration at  $i$  location designated  $a_i(t)$  and the sound pressure at  $k$  location  $p_k(t)$  when the point force is applied at  $j$  location  $f_j(t)$ . In experiments, one can measure  $H_{a_i, f_j}(f)$ , which is the FRF between  $f_j(t)$  and  $a_i(t)$ , and  $H_{p_k, f_j}(f)$  the FRF between  $f_j(t)$  and  $p_k(t)$ , respectively. The FRFs can be obtained, respectively, from simulation and experimental modal analysis (EMA) presented in Section 4.

One of the purposes in this study is to analytically predict the sound pressure response due to the impact striking force on the HSP.  $G_{p_k p_k}(f)$  is the auto power spectral density (PSD) function of  $p_k(t)$ , which sound spectrum is of interest.

### 3. Finite element model for harmonic sound plate

This section presents the construction of finite element (FE) model of HSP in considering the structure-only and the air-structure systems, respectively. Fig. 2(a) is the real structure of HSP. Fig. 2(b) is the FE model for the structure-only and Fig. 2(c) is for the air-structure system. The analysis is conducted by COMSOL. The HSP structure is built by the 8-node solid brick elements, and the air is modelled by the brick acoustic elements. Each node of the structural element has three degree-of-freedom (DOF) in terms of  $x$ ,  $y$  and  $z$  displacements, while the node of acoustic element contains the sound pressure DOF only. The fluid-structure-interface nodes contain both structural and acoustic DOFs.

In modal analysis for structure-only system, the undamped system solution is obtained, i.e. the normal mode solutions. The  $r$ -th structural natural frequency  $f_r$  and its corresponding structural mode shape  $\phi_r$  can be determined. It is noted that structural modal damping ratio can only be obtained from experiments. From harmonic response analysis, the system FRF between  $f_j(t)$  and  $a_i(t)$  referring to the experiment can also be simulated by applying unit point force at the  $j$  location and its direction and monitoring the  $i$  location's directional response accordingly.

For the air-structure system, the FE model of HSP and air is depicted as shown in Fig. 2(c). The air surrounding is assumed to be  $r=0.3$  m, and the outer surface is designated as free field boundary. The structure surface nodes linked with the air elements are specified as the fluid-structure-interface nodes. By examining Eq. (3) for the air-structure system equation, there are the effects of vibro-acoustic coupling matrix  $[R]$  in the cross term of the system mass matrix and stiffness matrix; therefore, the complex mode analysis is presumed. The air-structure system modal parameters can be obtained as  $\bar{f}_r$  and  $\bar{\phi}_r$ . The system mode shapes contain two parts of solutions. One is the structural displacement mode shapes  $\bar{\phi}_{r(s)}$ , and the other is the acoustic mode shapes in terms of sound pressure mode shapes  $\bar{\phi}_{r(a)}$ .

The harmonic response analysis is also performed on the air-structure system by applying force at the  $j$  location referring to the experiments, and then the system response at the structure and the air can be, respectively, obtained. In particular, the sound pressure spectrum can be calculated and compared with the measured one.

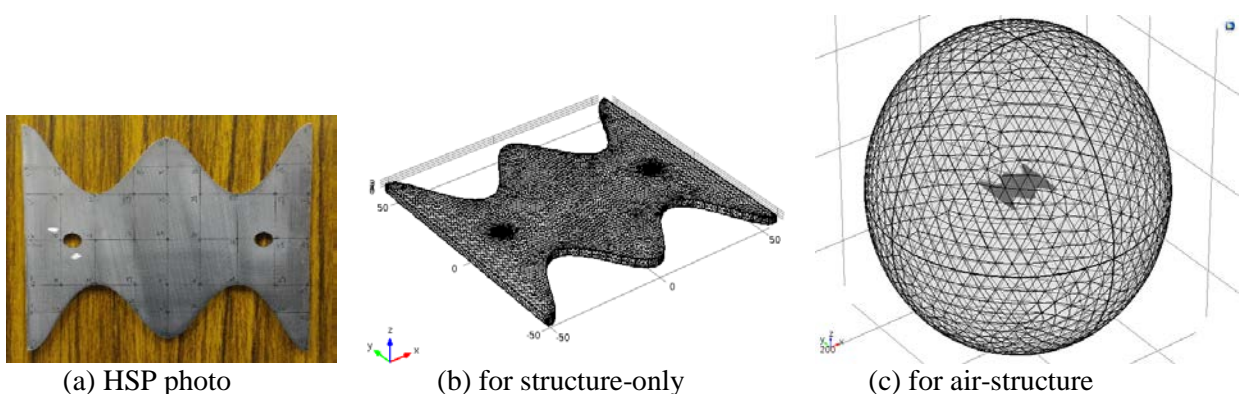


Figure 2: Harmonic Sound Plate (HSP) structure and its FE models.

## 4. Experimental modal analysis on harmonic sound plate

This section shows the conventional experimental modal analysis (EMA) on the HSP to experimentally determine the system modal parameters. Fig. 3(a) shows the experimental setup and Fig. 3(b) show the grid points on the HSP. First, the structural FRF  $H_{a_i, f_j}(f)$  between  $f_j(t)$  and  $a_i(t)$  can be obtained by moving the impact hammer and fixed the accelerometer at  $i=17$  to measure the  $z$ -direction force and acceleration. Then, the post processing is done by modal parameter extraction software ME'scopeVES to determine the structural modal parameters, including natural frequencies, displacement mode shapes and modal damping ratios. The microphone sensor is also applied to measure the system FRF between  $f_j(t)$  and  $p_k(t)$ . By fixed the microphone location and moving the impact hammer, a series of FRFs can be measured and used to extract the air-structural modal parameters.

It is noted that the HSP structure is actually the air-structure system. Either using the accelerometer or the microphone as the sensor to perform EMA on the HSP, we can get the air-structure system response with vibro-acoustic coupling effect. It is not possible to measure the structure-only system modal parameters in practice. However, we would also like to examine the air effect on the structural resonance for the real structure. Two experiments are carried out. One is to apply the accelerometer and microphone sensors simultaneously; the other is to apply the microphone only.

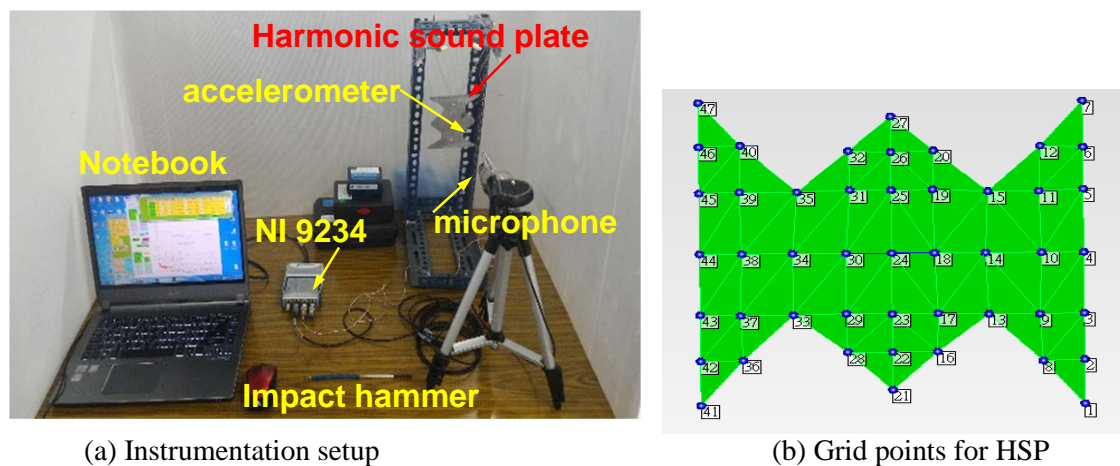


Figure 3: Experimental modal analysis on HSP.

## 5. Results and discussions

The model verification (MV) is to perform FEA and EMA on the HSP, respectively, and to compare the system FRF and modal parameters obtained from analysis and experiments. The agreement between analytical and experimental results indicates the successful simulation on the practical structure. Both the structure-only and air-structure systems will be discussed, respectively.

### 5.1 Structure-only system

Table 1 summarizes the modal parameters obtained from FEA and EMA. Because of the rigid body motion for the free-free HSP, the flexible body mode from FEA started at mode F07. Except mode F19 which is the  $y$ -direction mode is not measured, others are well compared with those from EMA by using the accelerometer. One can observe the average (AVG) and root-mean-square (RMS) of natural frequency error between FEA and EMA are 0.82% and 1.22%, respectively. The simulation in theoretical modal analysis (TMA) is in good agreement with EMA. The structural displacement mode shapes in  $(x, y)$  modes are also shown in Fig. 4(a) and 4(b) in order from FEA and EMA, respectively. The physical meaning of mode shapes for the HSP can be well interpreted.

Table 1: Modal parameters for structure field system.

FEA		EMA by acc.		Frequency difference (Hz)	Frequency Error (%)	Damping ratio (%)	Physical meaning of mode shape (x, y)
mode	Natural Frequency (Hz)	mode	Natural Frequency (Hz)				
F07	966.2	E01	946.2	19.95	2.10	0.07353	(2,2)
F08	1174.6	E02	1173.1	1.5	0.12	0.06310	(3,1)
F09	1810.5	E03	1768.6	41.9	2.36	0.09735	(3,2)
F10	2348.8	E04	2338.6	10.2	0.43	0.06091	(1,3)
F11	2368.9	E05	2366.8	2.1	0.08	0.04398	(2,3)
F12	3522.3	E06	3510.3	12.0	0.34	0.09855	(3,3)
F13	3888.0	E07	3821.2	66.8	1.74	0.49492	(4,1)
F14	4574.1	E08	4472.1	102.0	2.28	1.23550	(2,4)
F15	5215.9	E09	5207.2	8.7	0.16	0.07763	(1,4)
F16	6745.8	E10	6672.7	73.1	1.09	0.77482	(4,2)
F17	6941.9	E11	6879.8	62.1	0.90	0.11979	(3,4)
F18	7741.9	E12	7763.6	-21.7	-0.27	0.35521	(5,1)
F19	8696.0	--	--	--	--	--	y-direction mode
F20	8797.5	E13	8780.8	16.7	0.19	0.23804	(2,5)
F21	9314.7	E14	9321.3	-6.6	-0.07	0.07123	(3,5)
AVG					0.82		
RMS					1.22		

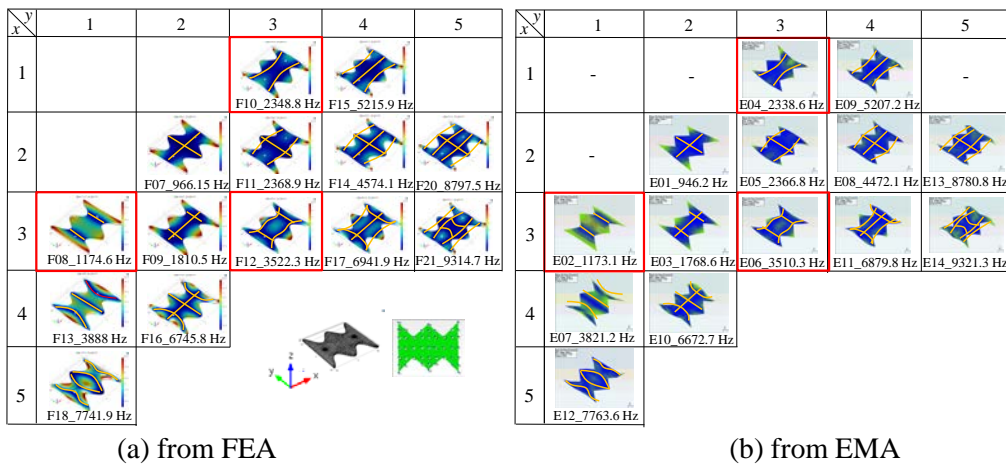


Figure 4: Comparison of structural displacement mode shapes.

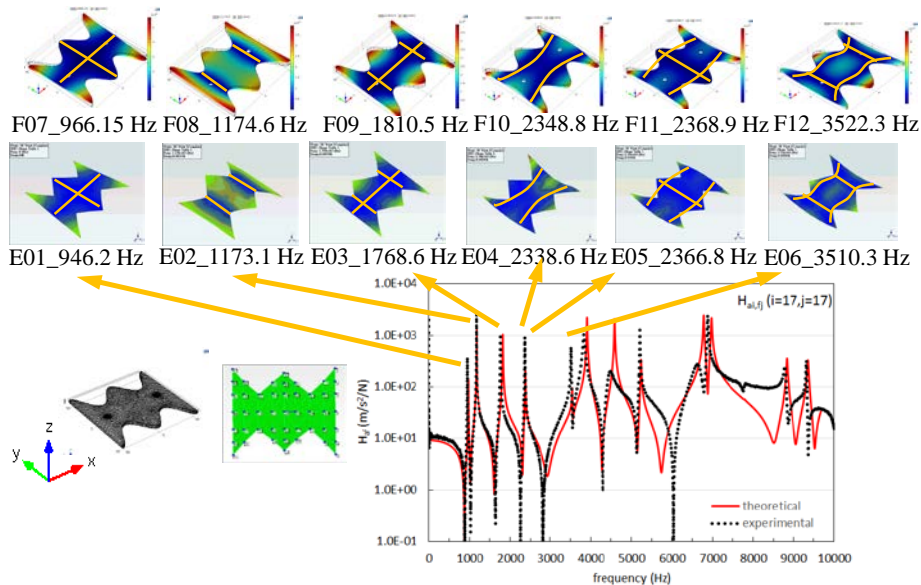


Figure 5: Frequency response function for structure and corresponding structural displacement mode shapes.

Fig. 5 shows the magnitude plots of FRF  $H_{a_i, f_j}(f)$  at  $(i=17, j=17)$ . Both the simulation and experimental curves agree very well. The first few mode shapes from FEA and EMA are also depicted on the top of corresponding resonant frequencies. In summary, the structural FRF and modal parameters can be well verified between FEA and EMA. The physical meaning of mode shapes are also visualized and shown good agreement.

## 5.2 Air-Structure system and percussion sound spectrum

The air-structure system is also analysed by performing both TMA and EMA, respectively. For examining the difference of natural frequencies between structure-only and air-structure systems, the TMA solutions by FEA are compared. There is only a slight difference within 0.9% between the structure-only natural frequencies  $f_r$  and the air-structure natural frequencies  $\bar{f}_r$ .

At this point, we still do not know the effect of air on natural frequencies of the air-structure system. The HSP attached with the accelerometer at  $i=17$  is also conducted EMA by the microphone. EMA on the HSP by using the accelerometer and microphone sensors, respectively, result in only within 5.6 Hz difference and less than 0.2% in maximum. This may conclude that the air-loading on the HSP is not significant, since the pitch frequency error for a note is within 0.3456%. For the HSP design purpose, the structure-only model can be sufficient for accurate design analysis. In addition, the mass effect of accelerometer should be carefully treated to avoid fault interpretation of the pitch frequency of HSP.

The main objective of this work is also to analytically predict the radiated sound pressure distribution for the HSP. By considering the air-structure system model as shown in Fig. 2(c), the radiated sound pressure spectrum can be obtained and compared with the experiment. Fig. 6 shows both the simulation and experimental sound spectrum of the HSP. The displacement mode shapes and acoustic mode shapes for the pressure contours and radiated pattern are shown for several resonant modes. It is noted that modes F08, F10 and F12, i.e.  $(x, y)=(3,1)$ ,  $(1,3)$  and  $(3,3)$ , respectively, are the designed harmonic sound with the frequency ratios up to 3. Those even modes such as  $(x,y)=(2,2)$  do not contribute much to the sound pressure response. The acoustic field analysis for the air-structure system is beneficial to visualize the sound pressure distribution in the air surrounding. The sound spectrum can be reasonably predicted and used for future sound quality evaluation analytically.

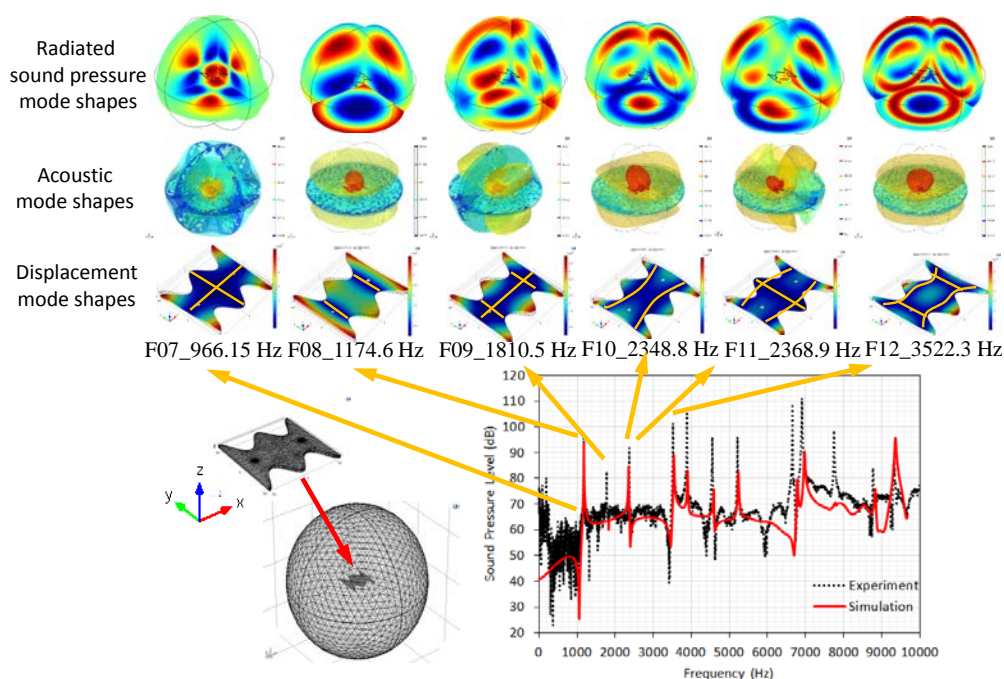


Figure 6: Sound pressure level for air-structure and corresponding acoustic mode shapes.

## 6. Conclusions

This paper presents the vibro-acoustic coupling analysis for the harmonic sound plate (HSP). Both modal analysis and harmonic response analysis are conducted on the structure-only and air-structure systems, respectively. To perform modal analysis on the system, one can obtain system modal parameters. For structure-only system, structural natural frequencies and displacement mode shapes can be determined and compared with experimental results in a good agreement.

For air-structure system, the structural natural frequencies are nearly the same, within 0.2% frequency difference for the HSP, as those of the structure-only system, although there are other acoustic modal frequencies. Both the structural displacement mode shape and the radiated sound pressure (acoustic) mode shapes in the air can be well interpreted. In particular, the acoustic mode shapes can help to visualize the sound radiation patterns for different modes.

The system frequency response function (FRF) for the acceleration with respect to the impact force in the structure system reveals very good agreement between analysis and experiments, while the FRF for the sound pressure with respect to the impact force in the air-structure system are also verified very well. This work details the vibro-acoustic coupling analysis and results in the satisfactory agreement with experiments, in particular for the HSP. The benefit for obtaining the percussion sound pressure spectrum due to the impact force on the HSP is that one can predict the sound field response and so forth to analytically examine the sound quality of HSP, which are potentially adopted as the percussion instrument.

## 7. Acknowledgement

The authors thanks to the financial support of this work by Ministry of Science and Technology under the grant No.: MOST 104-2221-E-020-033.

## REFERENCES

- 1 Wang, B. T. and Chien, H. M. *Board Capable of Generating a Harmonic Sound*, United States Patent No.: US 8,299,342 B2 (2012).
- 2 McLachlan, N., Nigjeh, B. K. and Hasell, A. The Design of Bells with Harmonic Overtones, *The Journal of Acoustical Society of America*, **114** (1), 505-511 (2003).
- 3 McLachlan, N., Adams, R. and Burvill, C. Tuning Natural Modes of Vibration by Prestress in the Design of a Harmonic Gong, *The Journal of Acoustical Society of America*, **131**(1), Pt.2, 926-934, (2012).
- 4 Pan, J. Acoustical Properties of Ancient Chinese Musical Bells, *Proceedings of Acoustics 2009*, Adelaide, Australia, (2009)
- 5 Yoo, J. and Rossing, T. D. Geometrical Effects on the Tuning of Chinese and Korean Stone Chimes, *The Journal of the Acoustical Society of America*, **120**(6), EL78-83, (2006).
- 6 Liu, Z. and Yi, C. The Analysis of Vibro-Acoustic Coupled Characteristics of Ball Mill Cylinder under Impact Excitation, *Modern Applied Science*, **2**(6), 37-40, (2008).
- 7 Wang, B. T., Chang, H. M., Huang, C.H., Yu, K.T. and Wu, Y.H. Vibro-Acoustic Coupling Analysis for Steel Chime Percussion Instrument, *Conference on 2015 Annual Meeting and 28th Symposium of Acoustical Society of Taiwan*, Taipei, Taiwan, Paper No.: A-03, (2015). (in Chinese)
- 8 Wang, B. T., Yu, K.T., Huang, C.H. and Wu, Y.H. Vibro-Acoustic Coupling Analysis and Verification of Crotale Percussion Instrument, *Proceedings of the 32<sup>nd</sup> National Conference on Mechanical Engineering, The Chinese Society of Mechanical Engineers*, Kaohsiung, Taiwan, Paper No.: B07-2198 (2015). (in Chinese)